Supporting Information

Novel Class of Water-Soluble Phosphonate Silver Cluster Assembled Material for Efficient Photoelectric Sensing and Photoacoustic Imaging

Sourav Biswas,[†a] *Anish Kumar Das,*[†a] *Akashdeep Nath,*[a] *Souradip Paul,*[b] *M. Suheshkumar Singh,*[b] *Sukhendu Mandal* [a *]

[a] *School of Chemistry, Indian Institute of Science Education and Research Thiruvananthapuram, Kerala 69551, India. E-mail: sukhendu@iisertvm.ac.in*

[b] *Biomedical Instrumentation and Imaging Laboratory, School of Physics, Indian Institute of Science Education and Research Thiruvananthapuram, Kerala 695551, India.*

[†]These authors contributed equally to this work.

Table of contents

Name	Description	Page No.
	Experimental	S3-S5
Table S1	Crystal data and structure refinement parameters	S6
Table S2	Theoretical energy calculation of monomer and dimers	S7
Fig. S1	The formula unit of the Ag_2 CAM.	S8
Fig. S2	QTAIM analysis of Argentophilic interaction	S9
Fig. S3	The one-dimensional growth of the Ag_2 CAM	S10
Fig. S4	The arrangement between two parallel apy linkers and two parallel linear cores	S11
Fig. S5	The attachment of $PhPO_3H^-$ with the core	S12
Fig. S6	The intermolecular H-bonding between P-O and P-O-H	S13
Fig. S7	Units for the theoretical energy calculation	S14
Fig. S8	The d-spacing of the crystal structure associated with the HRTEM	S15
Fig. S9	TEM and SEM images of Ag_2 CAM	S16
Fig. S10	The interlayer stacked (101) plane of the crystal structure associated with the SEM	S17
Fig. S11	SEM-EDAX of the Ag_2 CAM	S18
Fig. S12	XPS data of Ag_2 CAM	S19
Fig. S13	PXRD data of Ag_2 CAM	S20
Fig. S14	PXRD data after 3 months of Ag_2 CAM	S21
Fig. S15	TGA data of Ag_2 CAM	S22
Fig. S16	PXRD data of the heat treated crystal	S23
Fig. S17	^1H NMR of Ag_2 CAM in D_2O	S24
Fig. S18	^{31}P NMR of Ag_2 CAM in D_2O	S25
Fig. S19	Solid-state UV-vis absorbance spectra of Ag_2 CAM crystals	S26
Fig. S20	Theoretically predicted UV-vis absorbance spectra with oscillator strength	S27
Fig. S21	PA signal strength variation with the wavelength	S28
Fig. S22	Photography of the sample contained capillary tube inside the chicken breast and corresponding 2D MAP image	S29
Fig. S23	DPV experiment of Ag_2 CAM at room temperature	S30
	References	S31

Experimental

Materials

Silver nitrate ($AgNO_3$), adamantane thiol (AdmSH), silver trifluoroacetate (CF_3COOAg), phenyl phosphonic acid, and 4,4'-azopyridine were procured from Sigma-Aldrich. HPLC grade solvents- ethanol, acetonitrile and triethylamine (Et_3N) were purchased from Spectrochem.

Synthesis of $[Ag_2(PhPO_3H)_2(apy)_2]$

In a typical synthetic approach 0.1 mmol of $[AgS\text{-}Adm]_n$ and 0.1 mmol of CF_3COOAg were added together into the 6 mL of ethanol/acetonitrile mixture (1:1) and stirred for 2 h yielding a white suspension. Subsequently, 0.13 mmol of phenyl phosphonic acid and 0.13 mmol of 4,4'-azopyridine were sequentially added into the mixture and kept stirring for another 1 h. An orange color precipitate was formed and that was separated by centrifugation. Then the final orange color clear solution was kept at room temperature in a dark environment for 3 days. Crystals were obtained by slow evaporation of the solvent (Yield ~ 32 % on the basis of metal). The precursor, $[AgS\text{-}Adm]_n$ complex was synthesized by treating the equivalent amount of $AgNO_3$ and Adm-SH with Et_3N, by following the similar procedure of the synthesis of $[AgS\text{-}^tBu]_n$.[1] Crystallization is not successful without the silver thiol complex (even other silver salts do not produce the crystal), so adamantine thiol has a crucial role for the formation of this structure. ^1H NMR (500 MHz, D_2O in ppm): δ 8.83 (4H, d, pyridine, J= 3.7 Hz), 7.88 (4H, d, pyridine, J= 4 Hz), 7.77-7.73 (2H, m, benzene), 7.53-7.49 (3H, m, benzene). ^{31}P NMR (500 MHz, D_2O in ppm): δ 13.2256 (s).

X-ray Crystallography

The single-crystal X-ray data was collected on the Bruker Axs Kappa Apex II SC-XRD diffractometer with CCD detector by using monochromated MoK_α radiation (λ= 0.71073 Å) at 296 K. The crystal structure was solved by SHELXT 201449 and refined by the full matrix least-squares method using SHELXL 201850 present in the program suite WinGX (version 2014.1).[2, 3]

Computational Details

We calculated the optical absorption spectra of the Ag_2 CAM using time-dependent DFT with the Gaussian 09 program package.[4] The single-point calculation of the formula unit (extracted from the X-ray crystallographic data) was calculated with the B3LYP level utilizing the Los Alamos effective core potential (ECP) $LanL_2$-DZ for the Ag atoms and split-valence 6-31G(d) basis set for the rest of the atoms present.[5, 6] The argentophilic interaction between two Ag atoms was obtained with the Bader's AIM (Atoms in Molecules) approach using Multiwfn software package.[7] The obtained electron density (ED) and bond critical point (BCP) provides the strength of the interaction between two atoms. The Laplacian of the electron density, $\nabla^2\rho$ (rc) at BCP denotes the interaction pattern; negative value replys the covalent interaction, whereas positive value defines the non-covalent interaction.

The interaction energies (H-bonding and T-shaped π-π interaction) between the dimers were calculated using the equation,

$$\Delta E_{int}\,(\text{dimer}) = E_{\text{dimer}} - 2E_{\text{monomer}}$$

where, ΔE_{int} (dimer) = interaction energy of the dimer, E_{dimer} = total energy of the dimer, E_{monomer} = total energy of the monomer. These energy values were obtained using single-point calculation with B3LYP/$LanL_2$-DZ for the Ag atoms and split-valence B3LYP/6-31G(d) for other atoms in the Gaussian 09 program package.[4]

Instrumentation

A SHIMADZU UV-3800 spectrometer was used for measuring the absorbance spectra. XPS and UPS measurements have been done by using the Omicron Nano tech instrument (MgK_α radiation at 1253.6 eV). An X'pert PRO (PANalytics) powder diffractometer equipped with a Cu Kα (λ = 1.5405 Å) radiation source was used for the PXRD measurements. A Shimadzu SDT Q600 was used for the TGA with a heating rate of 10 $^oC\ min^{-1}$. A programmable temperature furnace (10 °C/min) with a constant flow of N_2 was used for heat treating the sample and keep the sample at 180 °C for 10 min and then cool at the specified rate, and then collected the PXRD data. Bruker Avance III, 500 MHz, ^1H NMR was used. For photocurrent response measurement the

sample solution was drop-casted on a patterned gold electrode with a gap of 1 mm. Then a keithley electrometer 6517b was used at room temperature for the data collection by applying a 10 V bias. The DPV measurement was carried out at 25 °C on a GC electrode in PBS buffer solution under N_2 atmosphere, and SCE was used as reference electrode in the analysis. PA-images were recorded by a home-built acoustic resolution photoacoustic microscope which is transmission configured Each sample was illuminated with an optical beam of 2.3 mm diameter, and a tuneable 100 Hz Innolas pulse lasers source repetition frequency of a 6 nsecs pulse width. A tightly focused V375-SU (Olympus) ultrasound transducer, 30 MHz (focal spot size 154 μm and focal length 19.10 mm) was used. To enhance the PA-signal strength, we adopted our reported optical pre-illumination technique in which CW-optical beam from a laser source (NPL52B, Thorlabs, Newton, New Jersey, USA; wavelength, 520 nm, power, 40 mW).[8] The chicken breast samples were collected from the super market.

Table S1. Crystal data and structure refinement parameters for Ag_2 CAM

Identification code	Ag_2 CAM
CCDC number	2102403
Empirical formula	$C_{16}H_{14}Ag_1N_4O_3P_1$
Formula weight	449.15
Temperature	296 (2) K
Wavelength	0.71073 Å
Crystal system	Triclinic
Space group	*P*-1
Unit cell dimensions	a = 7.4373(15) Å; b = 9.664(2) Å, c = 12.060(3) Å; α = 74.068(6)°; β = 82.863(6)°; γ = 83.792(6)°
Volume	824.5(3) $Å^3$
Z	2
Density (calculated)	1.809 mg/m^3
Absorption coefficient	1.343 mm^{-1}
F(000)	448
Crystal size	0.085 x 0.028 x 0.025 mm^3
Theta range for data collection	2.768 to 28.278 °.
Limiting indices	-9<=h<=9, -12<=k<=12, -16<=l<=16
Reflections collected	22398
Independent reflections	4051 [R(int) = 0.1228]
Completeness to theta = 25.242°	99.9 %
Refinement method	Full-matrix least-squares on F^2
Data / restraints / parameters	4051 / 0 / 227
Goodness-of-fit on F^2	1.028
Final R indices [I > 2sigma(I)]	R_1 = 0.0642, wR_2 = 0.1115
R indices (all data)	R_1 = 0.1304, wR_2 = 0.1360
Largest diff. peak and hole	1.053 and -0.941 e. $Å^{-3}$

Table S2. Theoretical energy calculation of monomer and dimers.

Molecules	**Energy (eV)**
Monomer	-117209.367328
Dimer 1	-234419.757232
Dimer 2	-234419.908

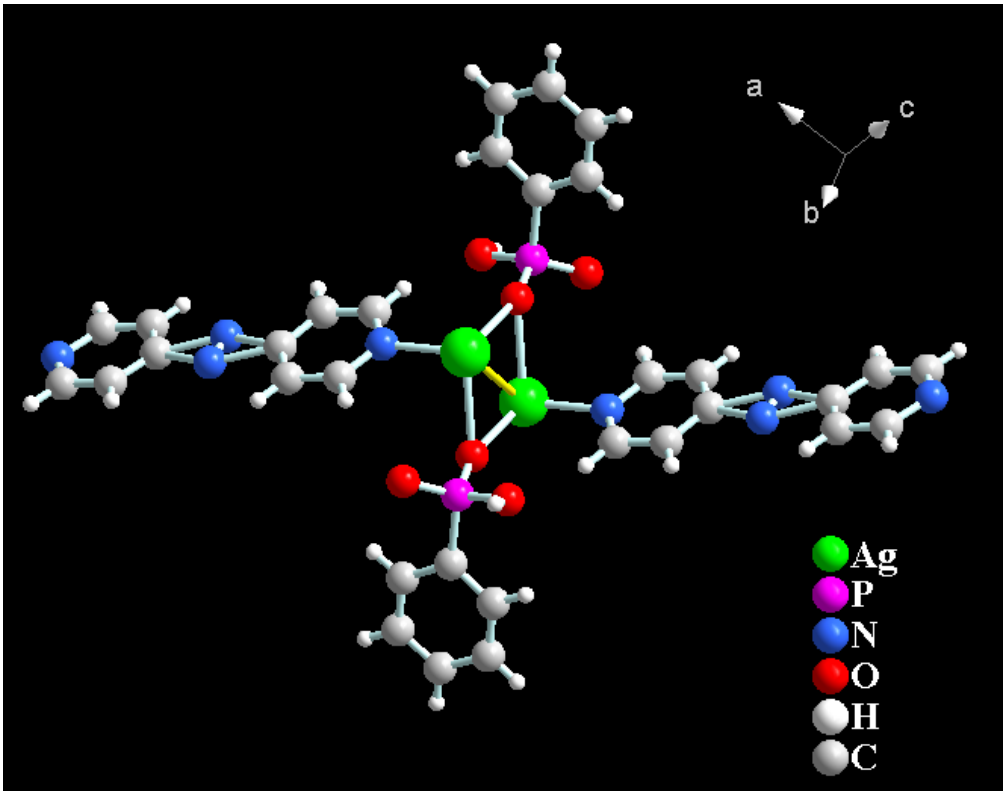

Fig. S1. Formula unit of the Ag_2 CAM.

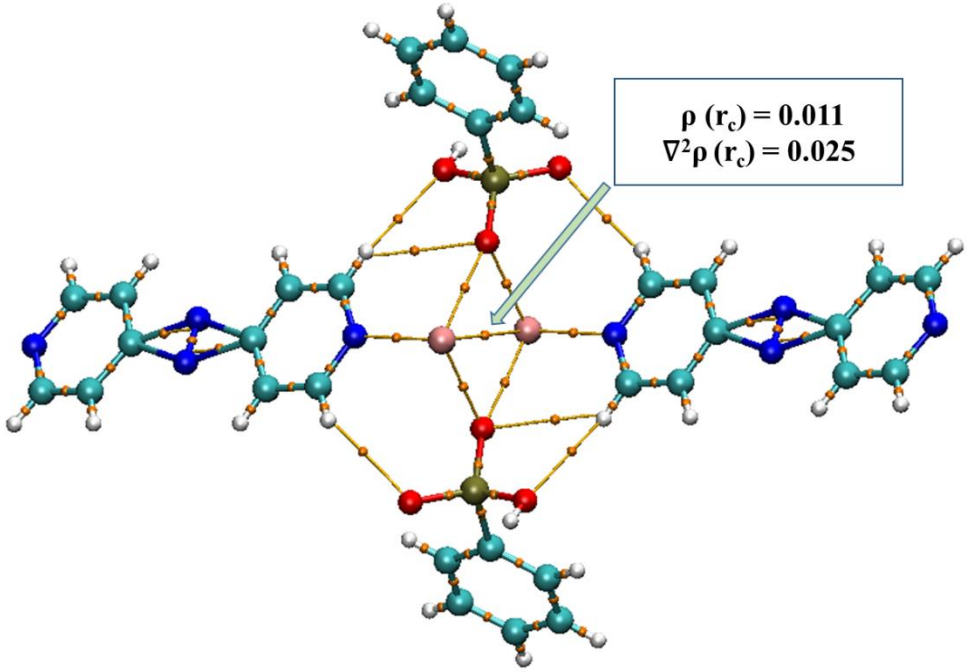

Fig. S2. QTAIM analysis of Ag_2 CAM with corresponding electron density and Laplacian value (in a.u.) at the bond critical point (BCP) along the Ag···Ag interaction path. The small orange dots represent the bond critical points.

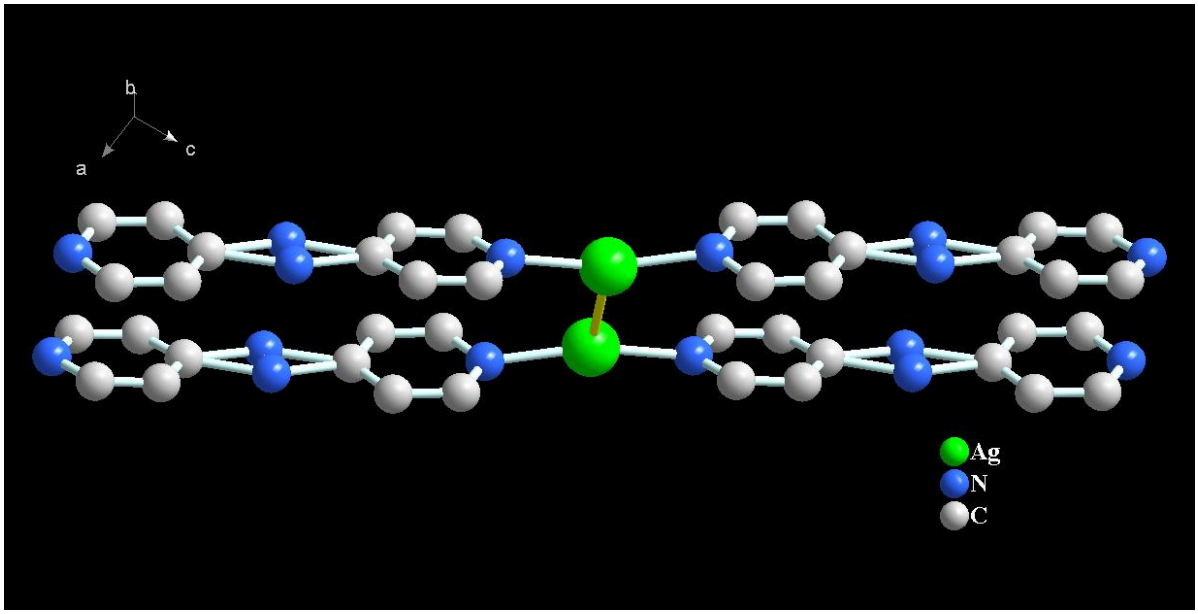

Fig. S3. One-dimensional growth of the Ag_2 CAM through the apy linker. All H atoms are omitted for clarity.

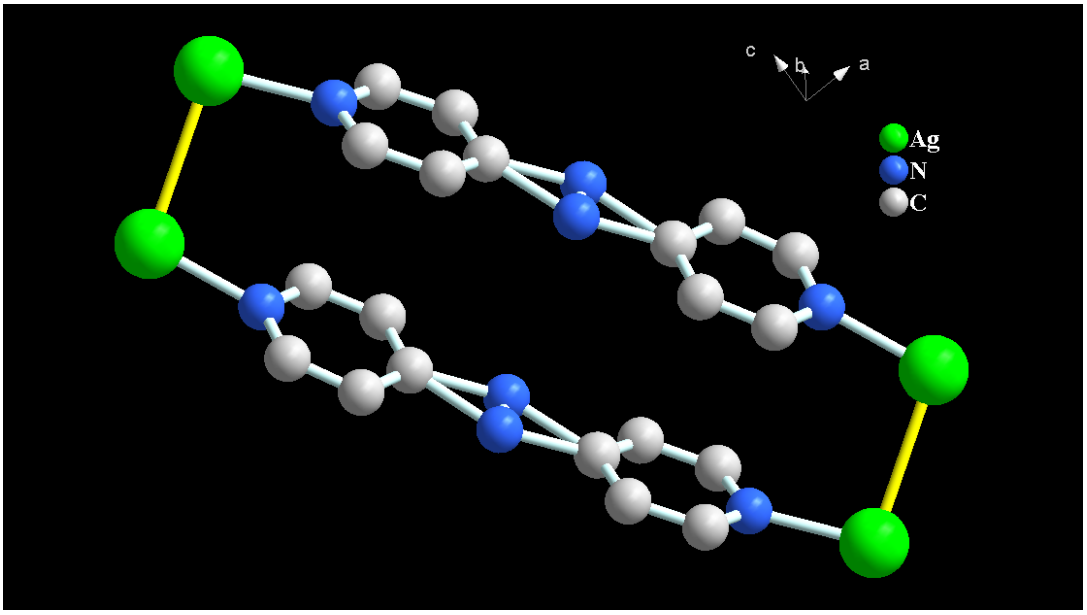

Fig. S4. Arrangement between two parallel apy linkers and two parallel linear cores construct the parallelogram geometry. All H atoms are omitted for clarity.

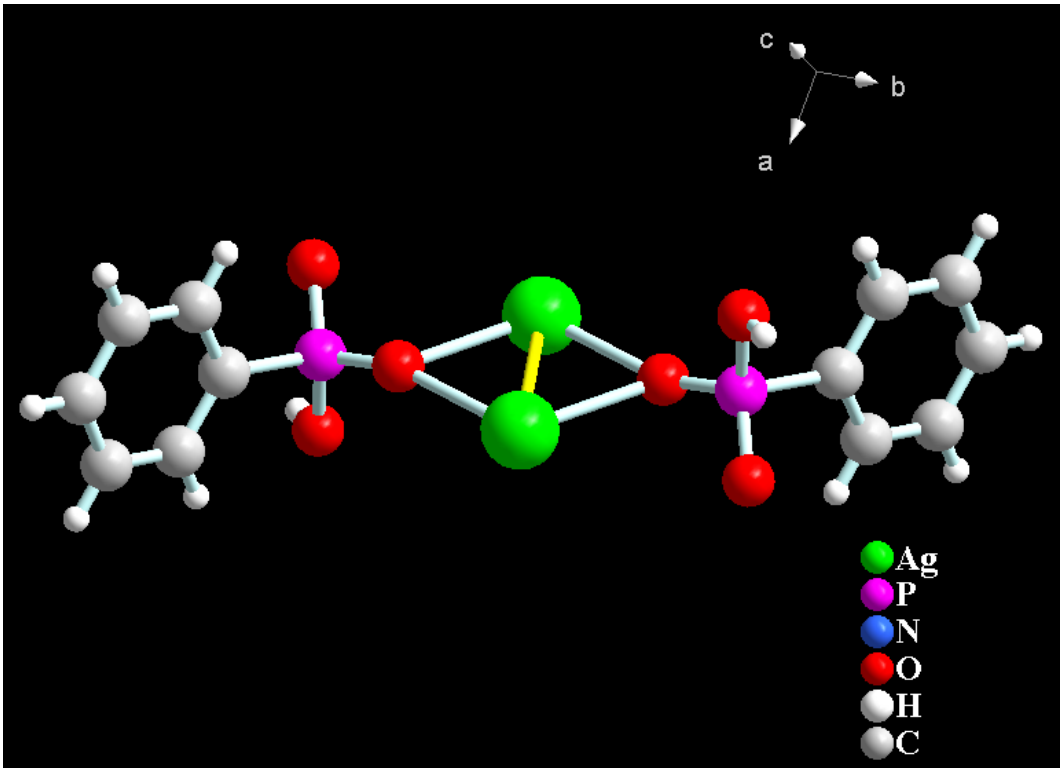

Fig. S5. Attachment of $PhPO_3H^-$ with the core from opposite site through the oxygen atom.

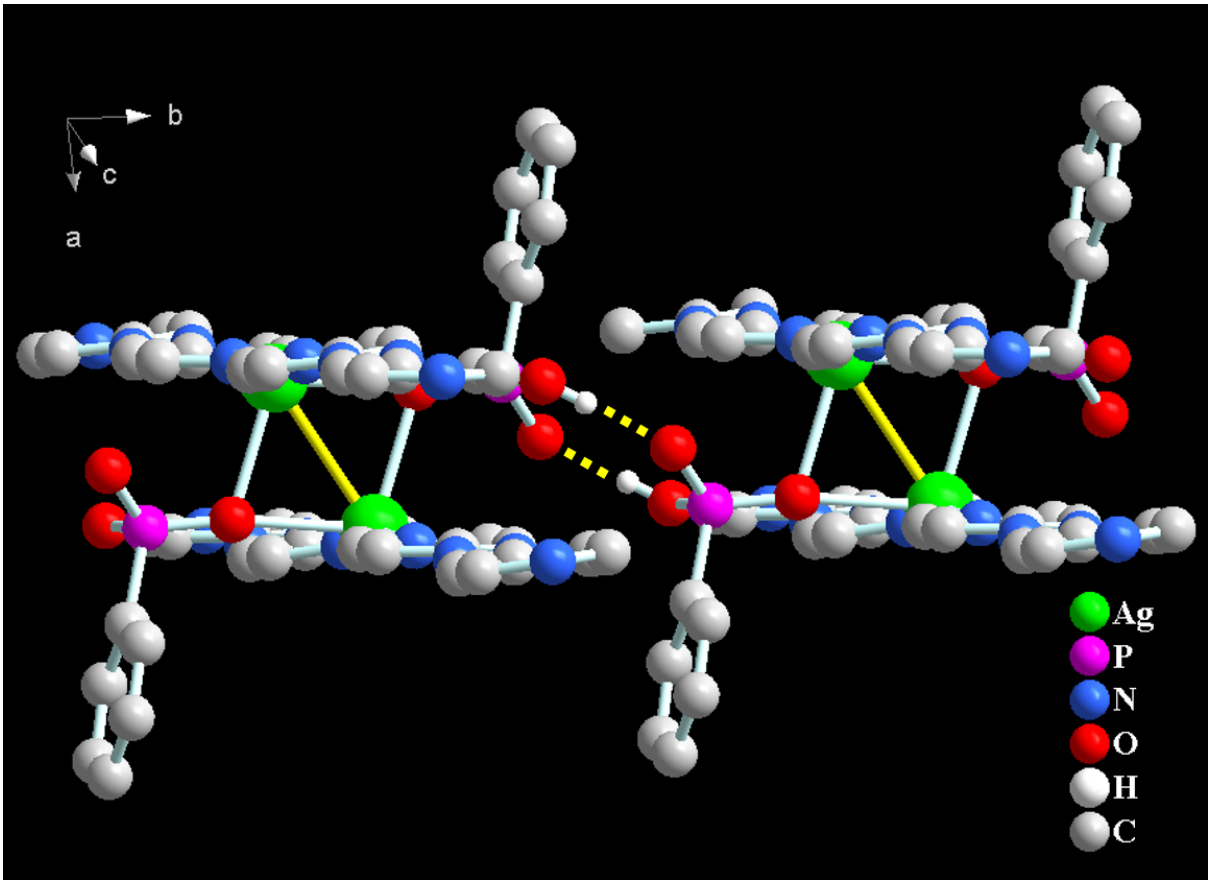

Fig. S6. Intermolecular H-bonding between P-O and P-O-H originating from the adjacent one-dimensional layers.

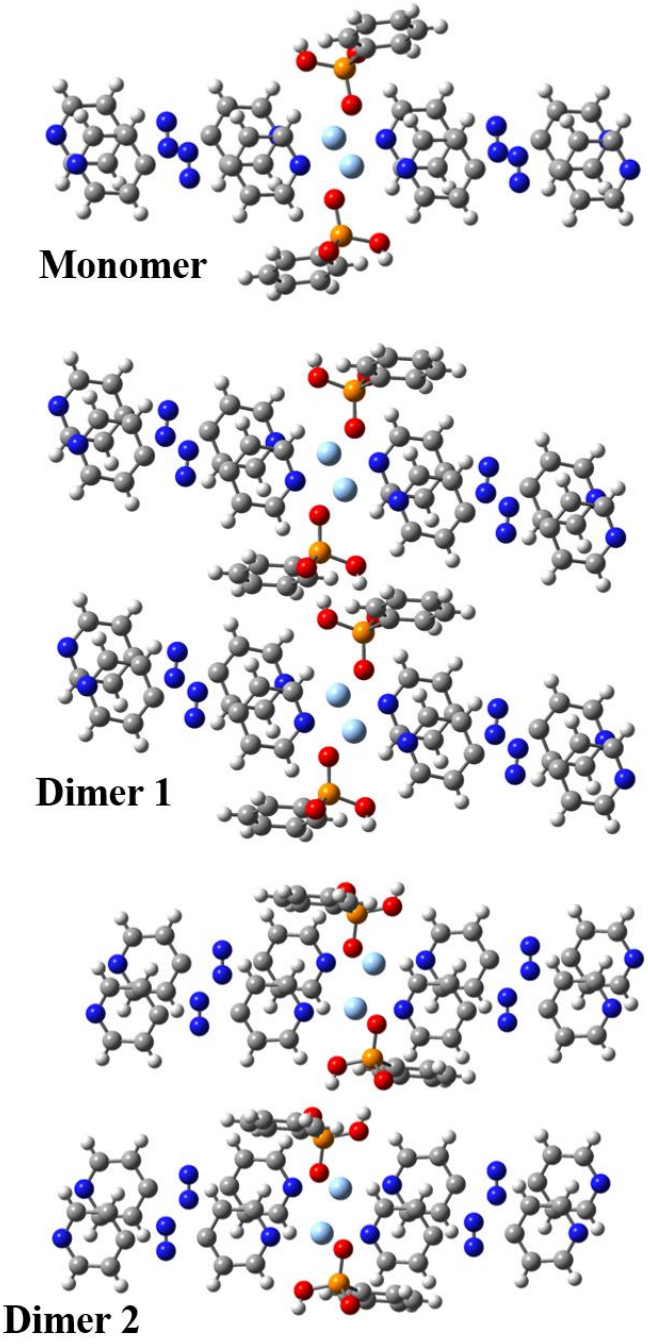

Fig. S7. Structural fragments for the theoretical energy calculation.

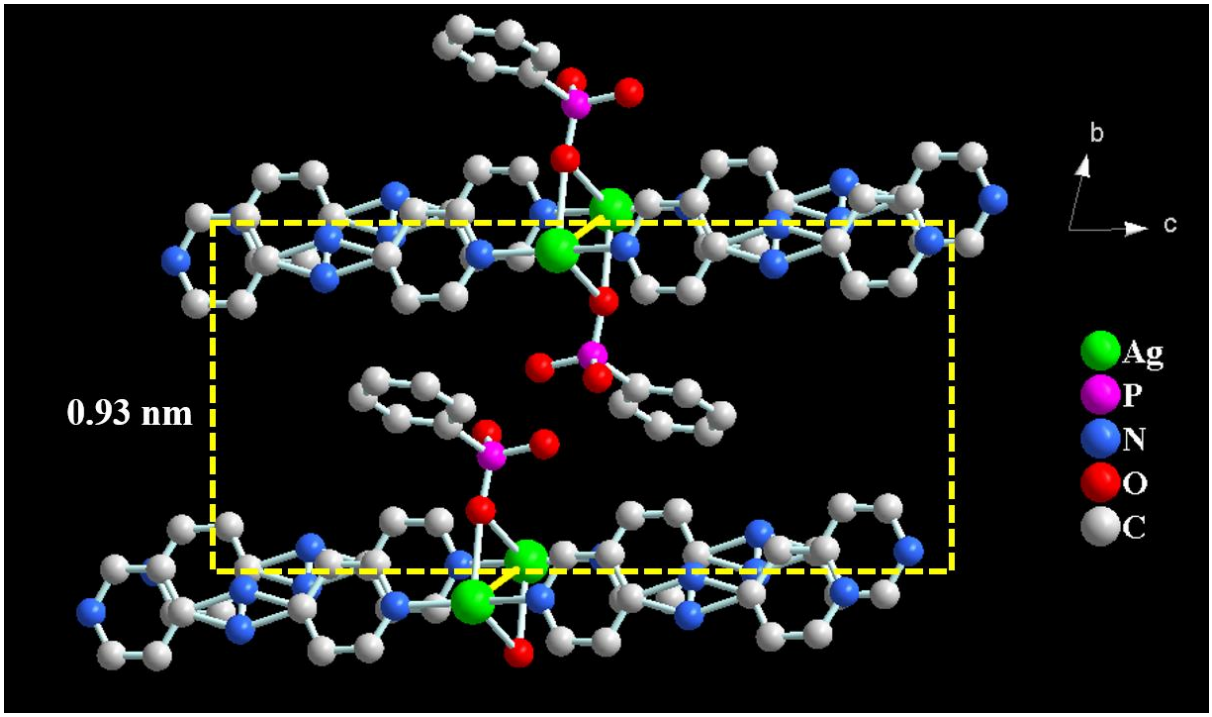

Fig. S8. d-spacing of the crystal structure which is further confirmed by the HRTEM image. All H atoms are omitted for clarity.

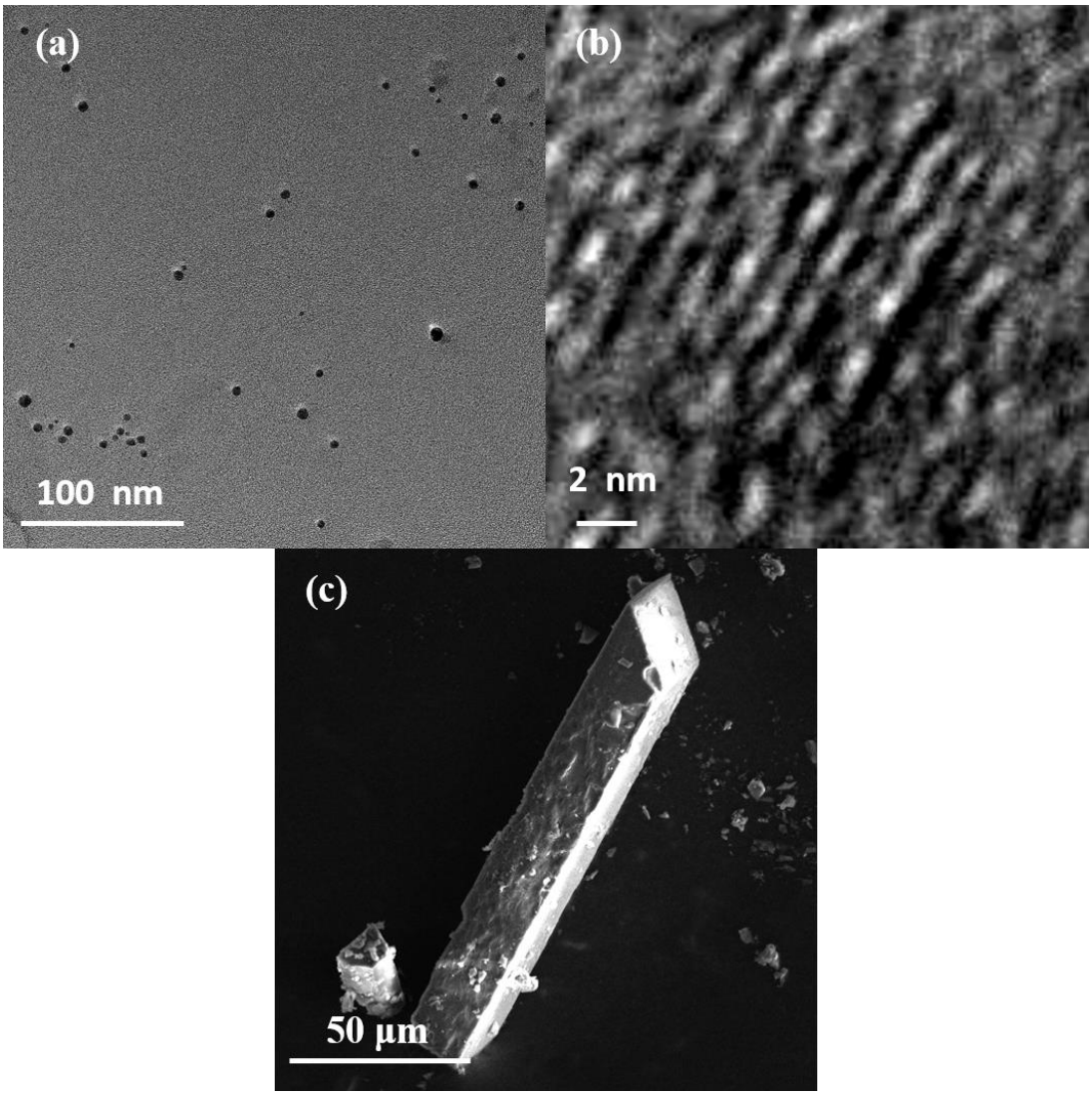

Fig. S9. (a) TEM image, (b) HRTEM image of drop-casted Ag_2 CAM and (c) SEM micrograph of the Ag_2 CAM crystals.

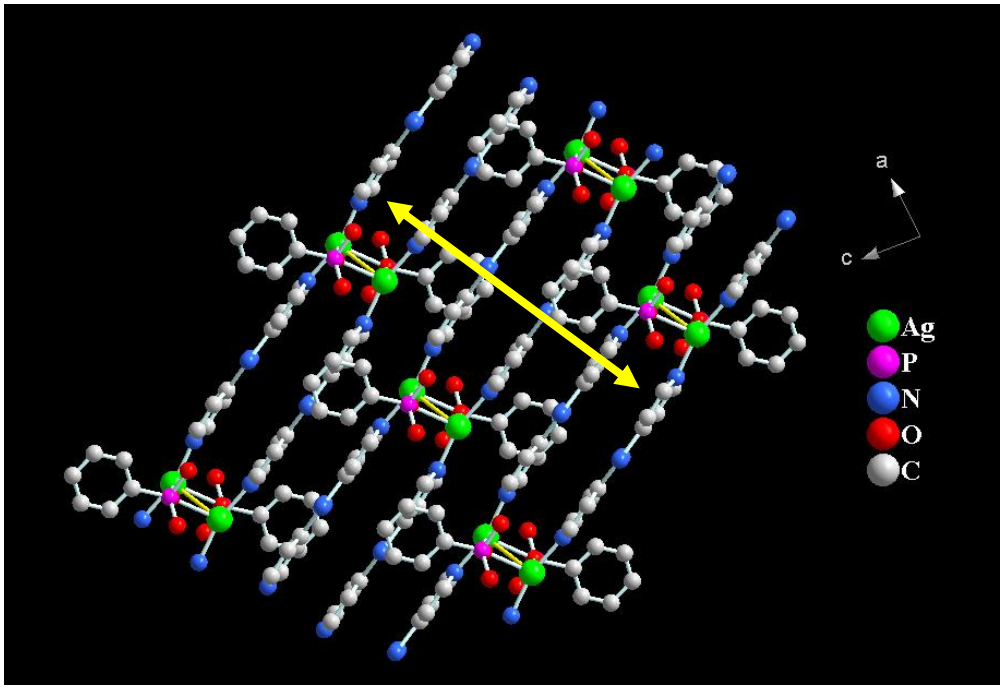

Fig. S10. Interlayer stacked (101) plane of the crystal structure corroborated with the SEM image. All H atoms are omitted for clarity.

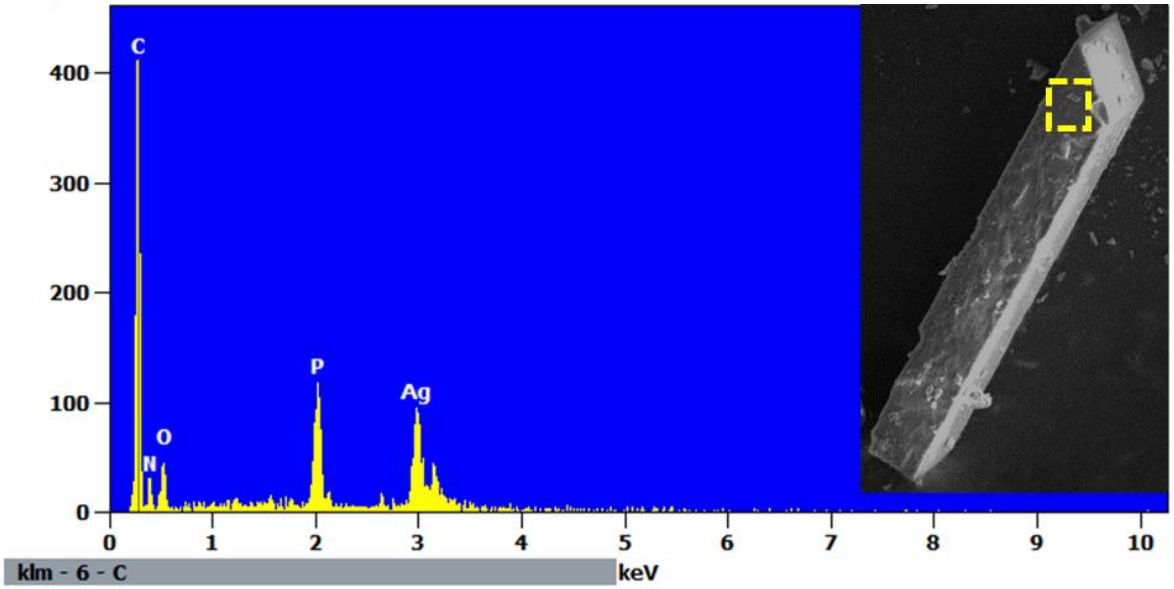

Fig. S11. Elemental analysis of the Ag_2 CAM by the SEM-EDS.

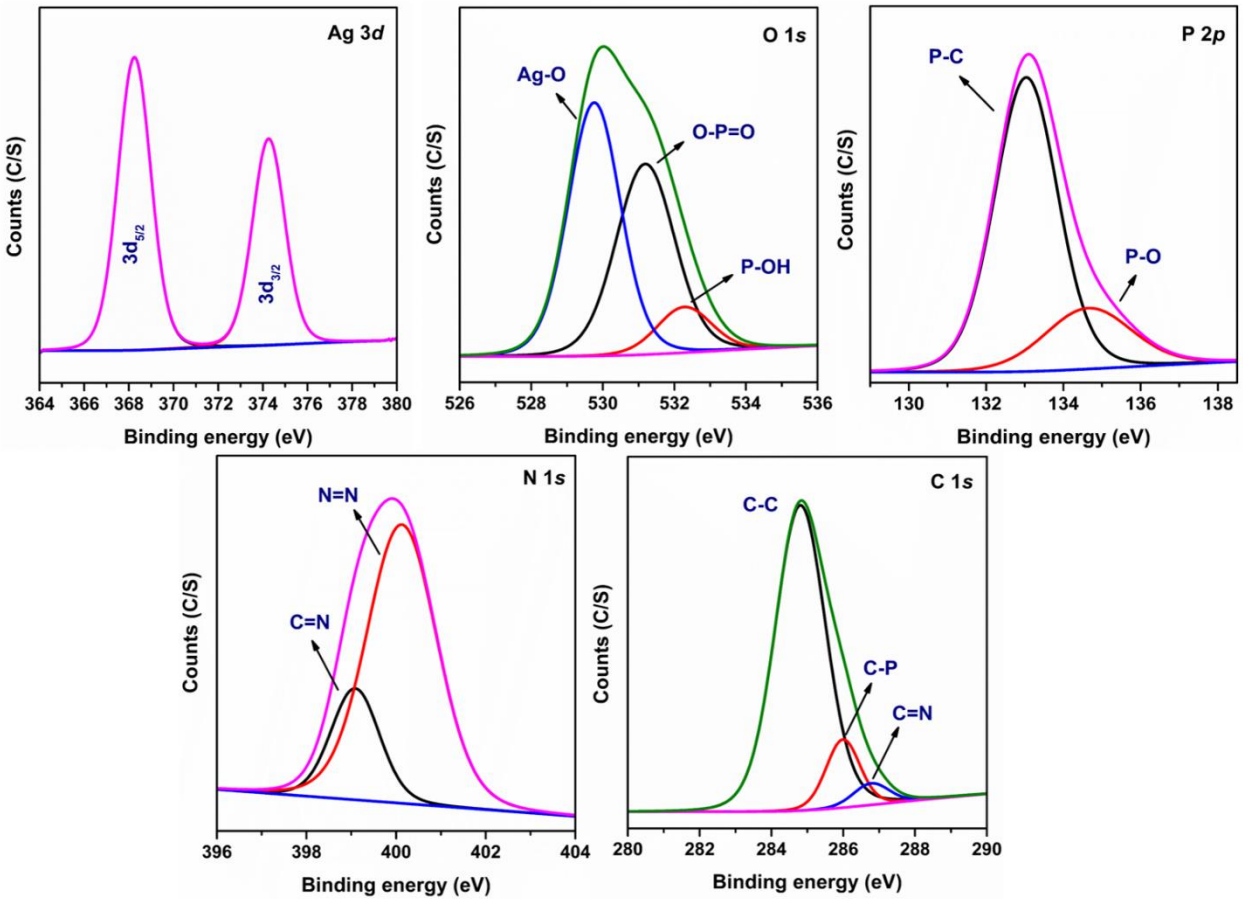

Fig. S12. XPS analysis of Ag_2 CAM.

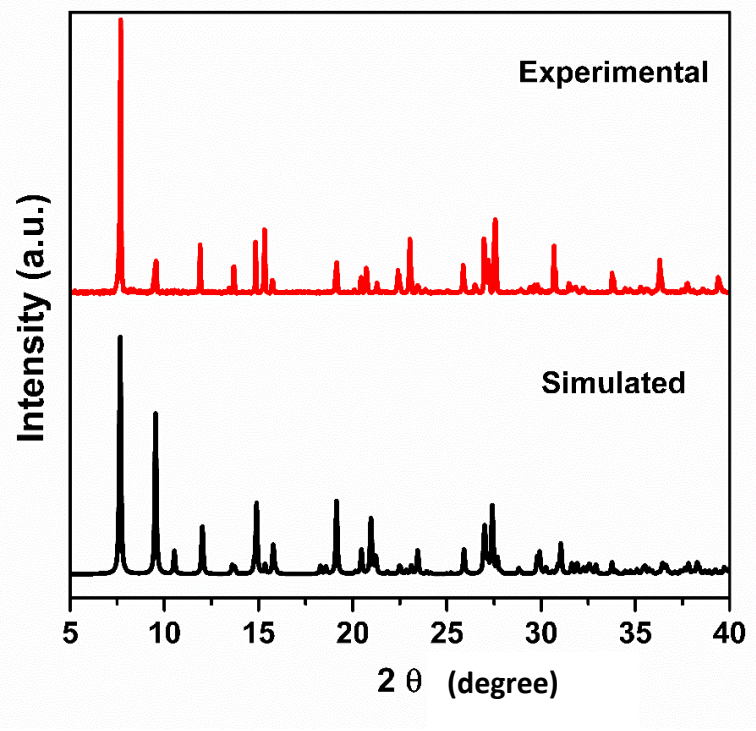

Fig. S13. PXRD data of the Ag_2 CAM, d-spacing of (010) plane is 0.93 nm.

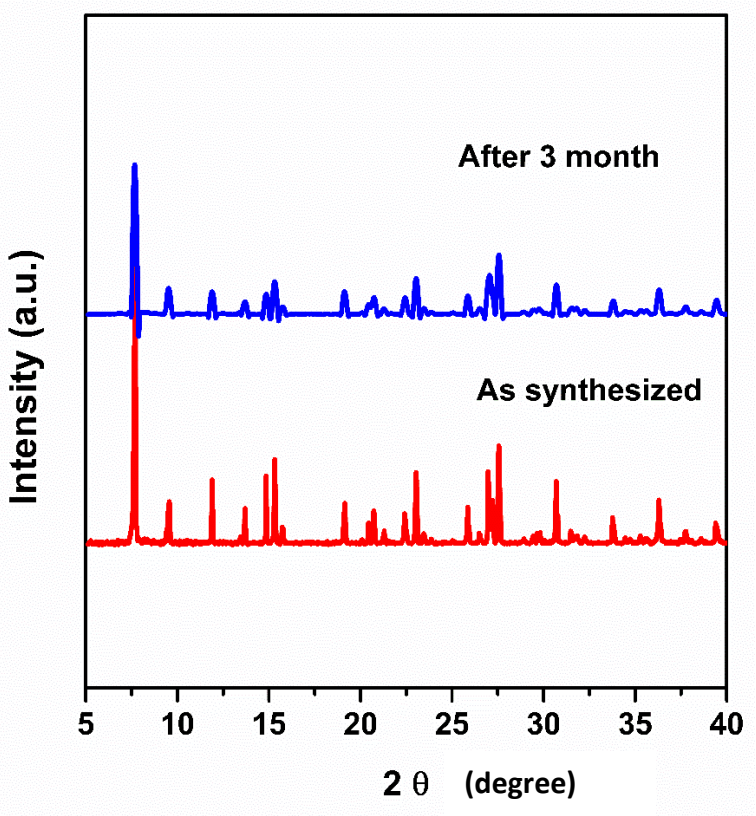

Fig. S14. PXRD data after 3 months of synthesis.

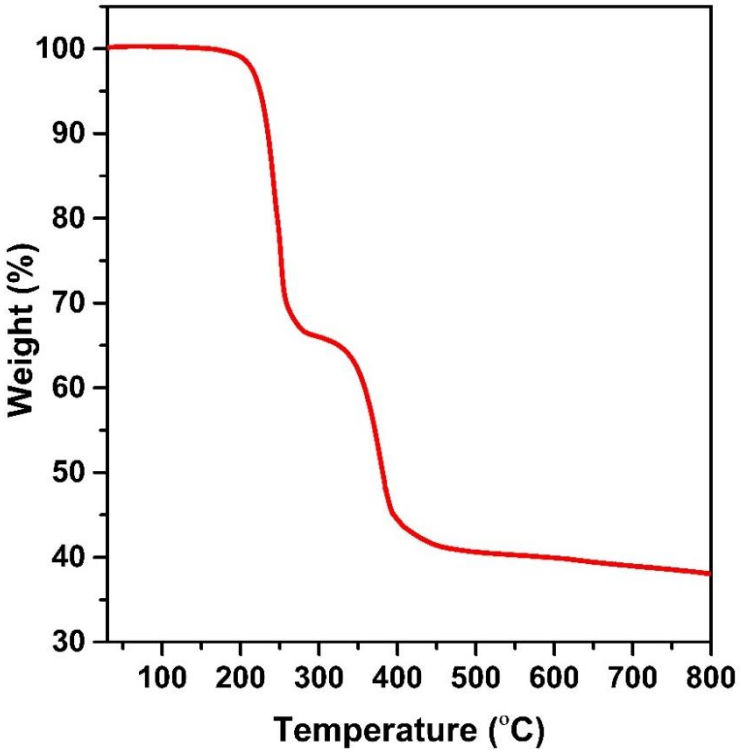

Fig. S15. TGA data of the Ag_2 CAM showing the thermal stability up to 200 ºC.

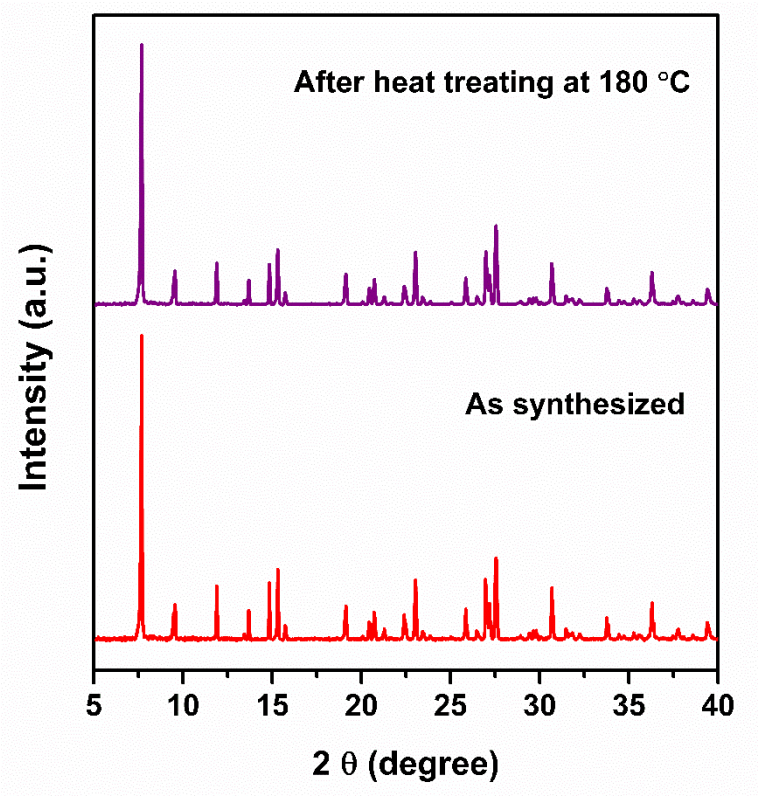

Fig. S16. PXRD data of the heat treated crystal.

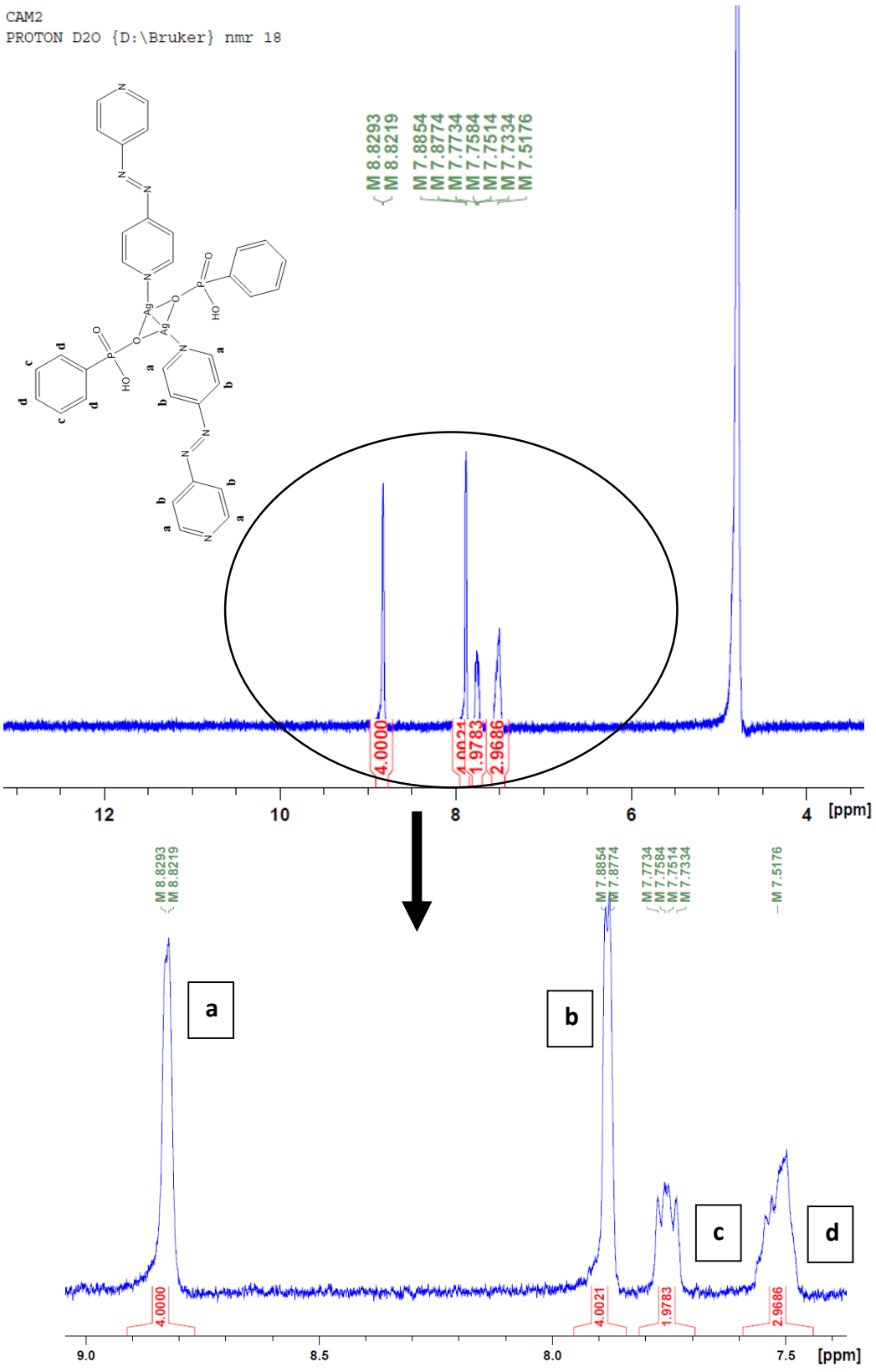

Fig. S17. ^{1}H NMR of Ag_2 CAM in D_2O.

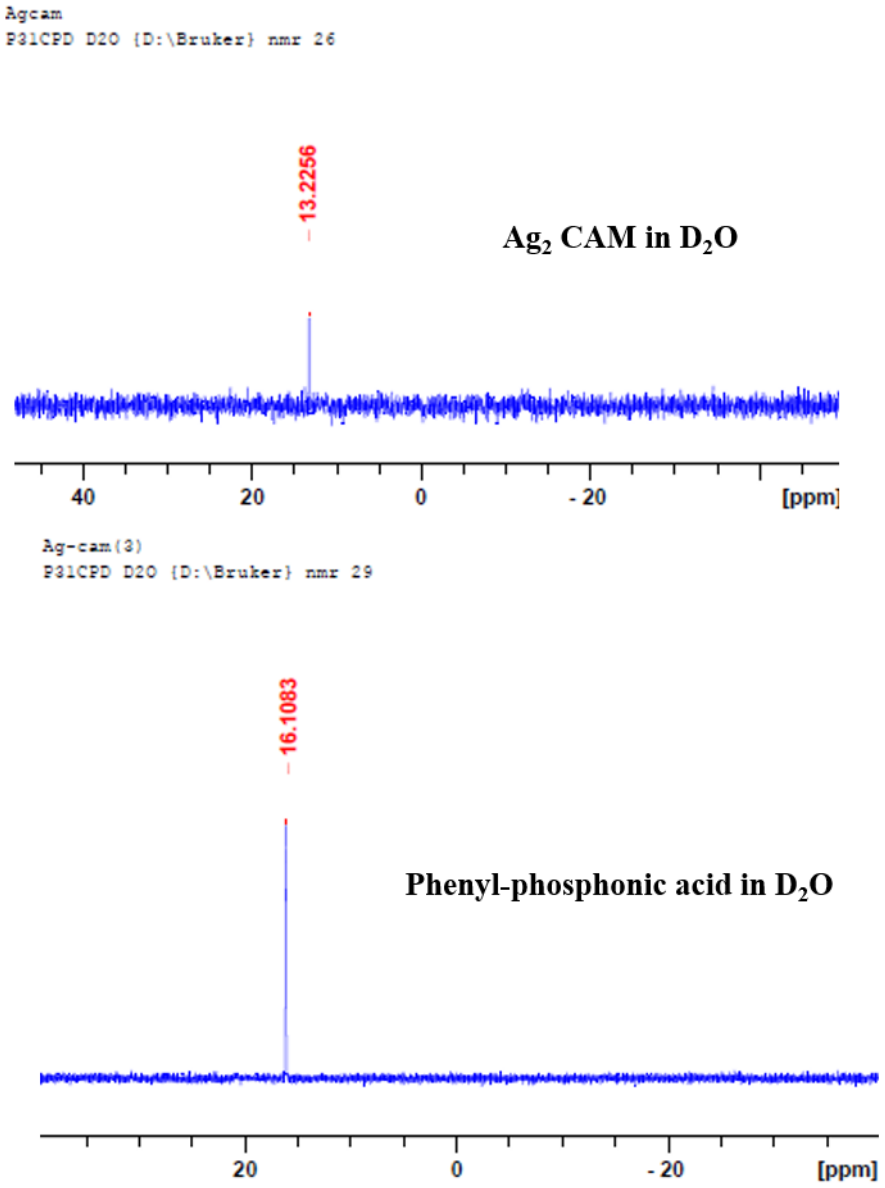

Fig. S18. ^{31}P NMR of Ag_2 CAM in D_2O.

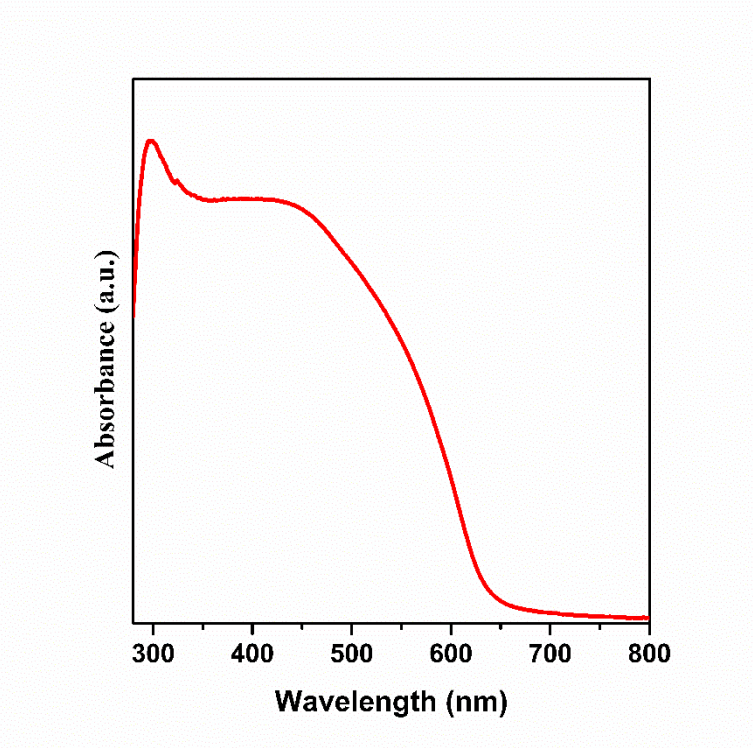

Fig. S19. Solid-state UV-vis absorbance spectra of Ag_2 CAM.

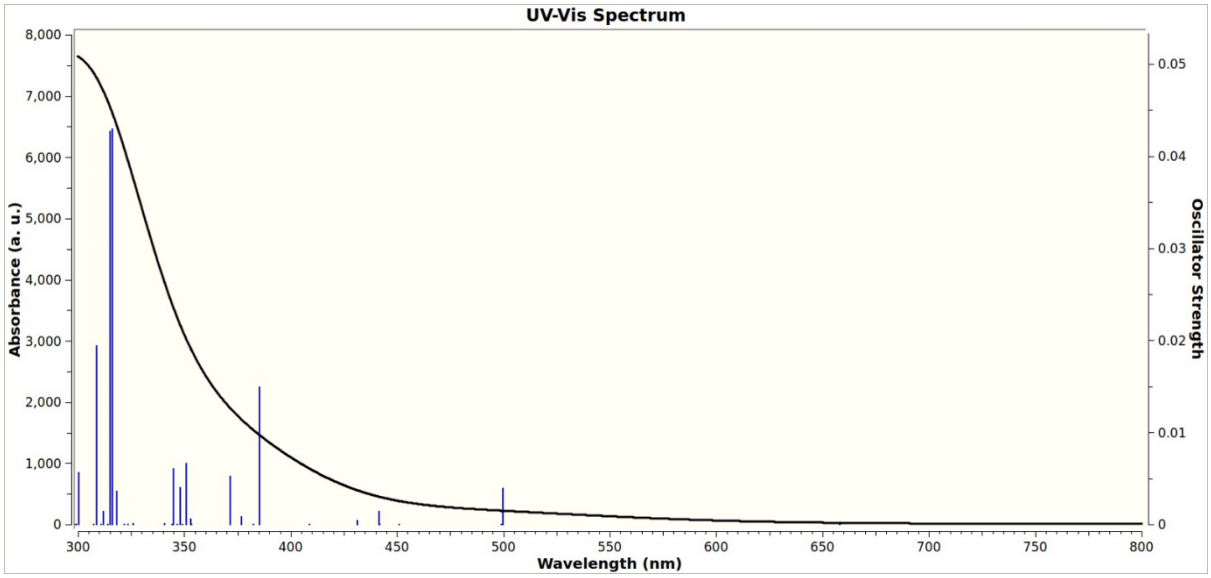

Fig. S20. Theoretically predicted UV-vis absorbance spectra with oscillator strength.

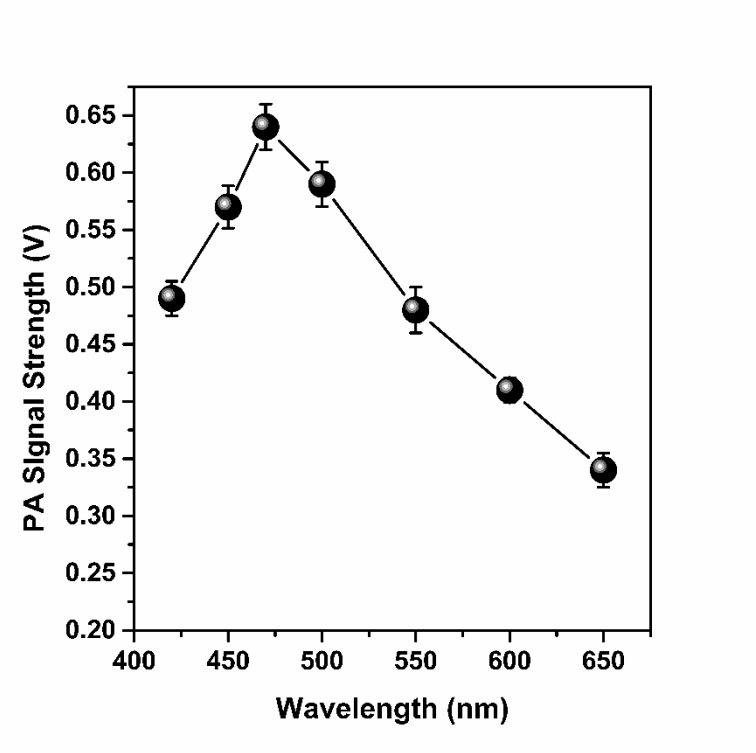

Fig. S21. PA signal strength variation with the wavelength.

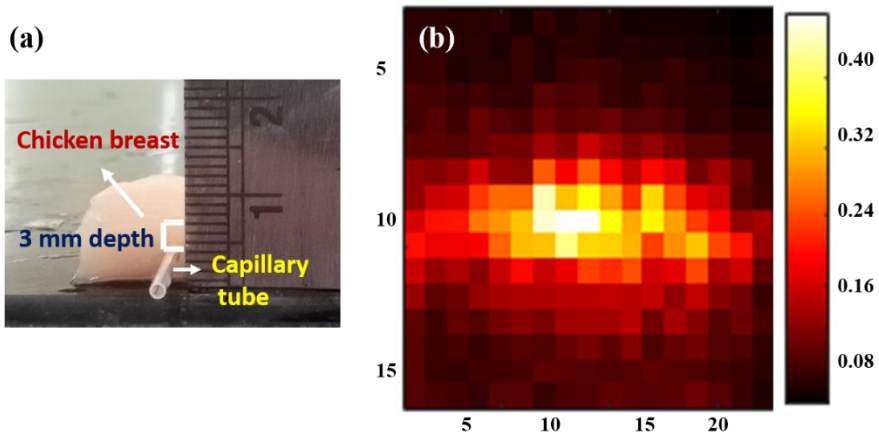

Fig. S22. (a) Photograph of sampled contained capillary tube inside the chicken breast tissue at 3 mm depth, (b) corresponding 2D MAP image of the Ag_2 CAM embedded inside the chicken breast tissue.

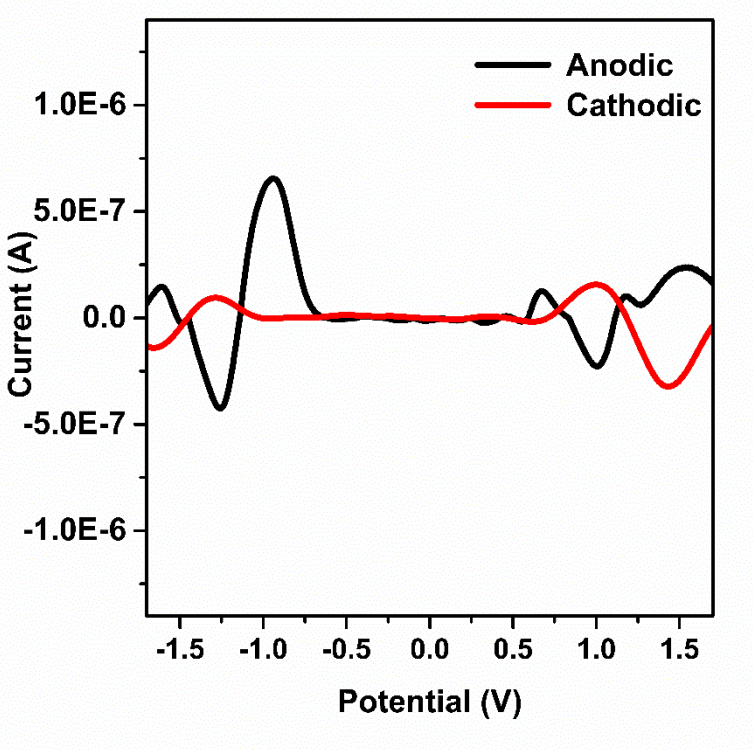

Fig. S23. DPV experiment of Ag_2 CAM at room temperature.

References

1 G. Li, Z. Lei and Q.-M. Wang, *J. Am. Chem. Soc.*, 2010, ***132***, 17678-17679.

2 G. M. Sheldrick, *Acta Crystallogr., Sect. C: Struct. Chem.*, 2015, ***71***, 3-8.

3 G. M. Sheldrick, *Acta Crystallogr., Sect. A: Found. Adv.*, 2015, ***71***, 3-8.

4 M. J. Frisch, G. W. Trucks, H. B. Schlegel, G. E. Scuseria, M. A. Robb, J. R. Cheeseman, G. Scalmani, V. Barone, G. A. Petersson, H. Nakatsuji, X. Li, M. Caricato, A. V. Marenich, J. Bloino, B. G. Janesko, R. Gomperts, B. Mennucci, H. P. Hratchian, J. V. Ortiz, A. F. Izmaylov, J. L. Sonnenberg, Williams, F. Ding, F. Lipparini, F. Egidi, J. Goings, B. Peng, A. Petrone, T. Henderson, D. Ranasinghe, V. G. Zakrzewski, J. Gao, N. Rega, G. Zheng, W. Liang, M. Hada, M. Ehara, K. Toyota, R. Fukuda, J. Hasegawa, M. Ishida, T. Nakajima, Y. Honda, O. Kitao, H. Nakai, T. Vreven, K. Throssell, J. A. Montgomery Jr., J. E. Peralta, F. Ogliaro, M. J. Bearpark, J. J. Heyd, E. N. Brothers, K. N. Kudin, V. N. Staroverov, T. A. Keith, R. Kobayashi, J. Normand, K. Raghavachari, A. P. Rendell, J. C. Burant, S. S. Iyengar, J. Tomasi, M. Cossi, J. M. Millam, M. Klene, C. Adamo, R. Cammi, J. W. Ochterski, R. L. Martin, K. Morokuma, O. Farkas, J. B. Foresman and D. J. Fox, Wallingford, CT, 2016.

5 P. J. Hay and W. R. Wadt, *J. Chem. Phys*, 1985, ***82***, 270-283.

6 P. J. Hay and W. R. Wadt, *J. Chem. Phys*, 1985, ***82***, 299-310.

7 T. Lu and F. Chen, *J. Comput. Chem.*, 2012, ***33***, 580-592.

8 A. Thomas, S. Paul, J. Mitra and M. S. Singh, *Sensors*, 2021, ***21***, 1190.